

High-energy neutrino production from photo-hadronic interactions of gamma rays from Active Galactic Nuclei at source

J.C. ARTEAGA-VELÁZQUEZ¹, ANGELO MARTÍNEZ²

¹ *Instituto de Física y Matemáticas, Universidad Michoacana, Morelia, Michoacan, Mexico*

² *Facultad de Ciencias Físico-Matemáticas, Universidad Michoacana, Morelia, Michoacan, Mexico*

arteaga@ifm.umich.mx

Abstract: Recent astronomical observations reveal that Active Galactic Nuclei (AGN) are sources of high-energy radiation. For example, the *Fermi-LAT* and *Hess* telescopes have detected gamma-ray emissions from the cores of several types of AGN's. Even more, the Pierre Auger observatory has found a correlation of ultra-high energy cosmic ray events with the position of Active Galactic Nuclei, such as Centaurus A. In this way, according to particle physics, a flux of high-energy neutrinos should be expected from the interactions of cosmic and gamma-rays with the ambient matter and radiation at the source. In this work, estimations of the diffuse neutrino flux from AGN's arising from interactions of the gamma radiation with the gas and dust of the sources will be presented.

Keywords: Diffuse Neutrino flux, Gamma ray emission, Photo-hadronic interactions, Active Galactic Nuclei

1 Introduction

Active Galactic Nuclei are among the most luminous extragalactic objects in the universe. Their emission covers all the electromagnetic spectrum, from radio up to the gamma-ray wavelengths and seems to have its origin in gravitational potential energy of matter falling inwards a supermassive black hole hidden deep at the source. It is around these supermassive objects where suitable conditions for particle acceleration may be found. Nowadays, it is believed that this process is behind the origin of the γ -ray emission seen from AGN's. In fact, there are two known particle physics scenarios for the production of γ -rays in AGN's, the so called hadronic and leptonic models. The former involves the acceleration and production of protons and atomic nuclei, whose interactions with the matter and radiation at the source lead to the production of secondary hadrons, which decay in γ -photons and neutrinos [1]. In this case, active galactic nuclei could also be important sources of high-energy neutrinos and cosmic rays. On the other hand, in the framework of the leptonic model, electrons and positrons are accelerated up to the relativistic regime producing gamma rays by radiative processes [2]. Although, no hadron acceleration up to the highest energies occurs, neutrinos are still produced in this scenario by means of secondary mechanisms induced by γ -ray collisions with the material and radiation of the source. In any case, no matter the mechanism of γ -ray production, the sole presence of this radiation implies the existence of at least a feeble flux of high-energy neutrinos coming from gamma-ray interactions at the source and its surroundings.

In reference [3], the diffuse flux of neutrinos from FR I and BL Lac type galaxies produced by photo-hadronic interactions of gamma rays during their way out the source and the host galaxy was investigated. In that work, in fact, it was shown that this particular flux is out of the reach of modern neutrino telescopes. Even more, in case that bigger neutrino detectors could be built, the detection of this diffuse ν flux would be difficult to achieve due to the presence of the strong atmospheric ν background. However, it was learned that high-energy neutrino emission is not

absent in AGN's at all and that, if neutrinos are ever detected from FRI and BL Lac galaxies, they would come from hadronic scenarios. In the present contribution, the research is extended to FR II galaxies. These objects have a bigger intrinsic absorption in X-rays than FR I galaxies [4], therefore, they offer more target material for ν -production by photo-hadronic interactions. Besides, from the *Fermi-LAT* surveys, it results that FR II galaxies with MeV – TeV emission are more γ -ray luminous than FRI type AGN's, which can also enhance neutrino emission by γ -ray collisions in those environments. However, their contribution to the diffuse flux of high-energy neutrinos in the universe could be strongly compromised due to the fact that the population of FR II seems to escape from the *Fermi-LAT* detection [5], which may be caused by an anisotropic emission from the source. If true, this phenomenon would favor the detection of FR II type galaxies with small jet inclination angles with respect to the observer's line of sight in the *Fermi-LAT* data [5]. The paper is organized as follows: First, a brief description of the calculation of the diffuse flux of neutrinos from individual sources is presented. Then, the γ -ray spectral luminosity of FR II objects is shown along with the associated neutrino flux for a single source. Next, a model for the matter distribution of the powerful radio galaxy Cygnus A is described. This is the closest FR II object to the Earth. And finally, the diffuse flux of neutrinos from photo-hadronic interactions of γ -photons from FR II galaxies is given.

2 The diffuse neutrino flux

The extragalactic flux of neutrinos (in units of $\text{s}^{-1} \cdot \text{sr}^{-1} \cdot \text{TeV}^{-1} \cdot \text{cm}^{-2}$) detected at Earth is estimated from the following expression:

$$\frac{d\Phi_{\nu}(E_{\nu}^{\circ})}{d\Omega^{\circ}} = \frac{c}{4\pi} \int_0^{z_{\max}} \frac{dz}{H(z)} \int_{\log_{10} \mathcal{L}_{\gamma}^{\min}}^{\log_{10} \mathcal{L}_{\gamma}^{\max}} d(\log_{10} \mathcal{L}_{\gamma}) \cdot \rho_{\gamma}(\mathcal{L}_{\gamma}, z) \cdot L_{\nu}[\mathcal{L}_{\gamma}, E_{\nu}^{\circ}(1+z)], \quad (1)$$

AGN	α
3C380	-2.51 ± 0.30
3C207	-2.42 ± 0.10
3C111	-2.54 ± 0.19
PKS0943	-2.83 ± 0.16

Table 1: Spectral indexes for the gamma-ray fluxes measured by *Fermi-LAT* from several FR II type objects [5].

where $L_\nu[\mathcal{L}_\gamma, E_\nu]$ is the neutrino spectral luminosity of a FR II type source localized at redshift z and characterized by an integrated γ -ray luminosity \mathcal{L}_γ in the interval from 100 MeV to 10 GeV. Here, $E_\nu = E_\nu^\circ(1+z)$ represents the neutrino energy at source and E_ν° , the redshifted energy as measured at Earth. On the other hand, $\rho_\gamma(\mathcal{L}_\gamma, z)$ is the gamma-ray luminosity function (GLF) of FR II sources per comoving volume dV_c and interval $d(\log_{10} \mathcal{L}_\gamma)$, as given by [6]. The Hubble parameter at z is represented by $H(z)$. Along the paper, a Λ CDM cosmology is assumed with $\Omega_\Lambda = 1 - \Omega_m = 0.74$. Integral limits are $z_{max} = 5$ [6] and $\mathcal{L}_\gamma^{min(max)} = 43(50) \text{ ergs/s}^{-1}$ (based on observations from FR II and FSRQ type objects performed by *Fermi-LAT* [5]).

3 Luminosities of FR II galaxies

As in reference [5], we assumed a power-law spectrum for the photon spectral luminosity at source, $L_\gamma(E_\gamma) = dN_\gamma/dt dE_\gamma = L \cdot E_\gamma^\alpha$. Measurements of the spectral slope, α , in the interval 100 MeV – 10 GeV were provided in [5] by the *Fermi-LAT* collaboration for a set of four FR II galaxies (see table 1). For our calculations, we adopted a standard FR II source with $\alpha = -2.57 \pm 0.18$, which corresponds to the mean value of the spectral index of the set of data in table 1 (the error represents the corresponding standard deviation of the data). We also add an energy cutoff around $E = 100 \text{ TeV}$, assuming conservatively that the leptonic model is at work. On the other hand, we will adopt the hypothesis that the γ -ray emission from FR II type galaxies is anisotropic to explain the small number of FR II objects detected by *Fermi-LAT* [5]. The main idea behind this hypothesis is that the γ -ray flux is born in the AGN jet as a result of Compton scattering of external photons by electrons, which produces a strong Doppler boosting and a narrow beaming cone of emission [5]. From the discussion at the beginning of this section and following [8, 9], the photon spectral luminosity per solid angle interval at the reference frame of the source galaxy will have the following form:

$$\frac{dL_\gamma(E_\gamma, \theta, i)}{d\Omega} = N \cdot \eta(\theta, i) \cdot \left(\frac{E_\gamma}{\text{TeV}} \right)^\alpha \cdot e^{-(E_\gamma/10^2 \text{ TeV})}, \quad (2)$$

where i is the angle between the jet direction of the AGN and the line of sight to the observer and θ , the angle between the jet axis and the direction of the emitted photon. Here, N is a normalization factor chosen in such a way that for an observer with an angle of view i , the measured integrated luminosity per interval of solid angle at source that would be measured in that direction is $\mathcal{L}_\gamma/4\pi$. On the other hand,

$$\eta(\theta, i) = \frac{1}{4\pi} \left[\frac{\delta_D(\theta)}{\delta_D(i)} \right]^{4+2a} \left(\frac{\mu_i}{\mu_\theta} \right) \left(\frac{1+\mu_\theta}{1+\mu_i} \right)^{2+a}, \quad (3)$$

with $\delta_D(\theta) = 1/[\Gamma(1 - \mu_\theta \beta)]$, the Doppler factor, and $\mu_\theta = \cos(\theta)$. Similar expressions apply for μ_i and $\delta_D(i)$.

In the above equation, Γ is the Lorentz factor of the material in the jet and $\beta = \sqrt{1 - 1/\Gamma^2}$. We will take $\Gamma = 5$ and 10. Finally, $a = -\alpha - 1$.

For the calculation of the neutrino luminosity, only photo-hadronic interactions are taken into account. Contributions from μ -pair production in γ -ray interactions with matter and photons will be neglected due to their lowest cross-section. The target for the gamma radiation will be the nucleons of the gas and dust of the AGN and its host galaxy. We will assume that this material is composed of protons with energies well below 100 MeV. In this way, they will be considered at rest during the calculations of the γP collisions. The neutrino spectral luminosity per solid angle interval along a given direction θ from the jet axis is given by the expression

$$\frac{dL_\nu(E_\nu, \theta, i)}{d\Omega} dE_\nu = \Sigma_H(\theta) \int_{E_{\gamma,i}}^{E_{\gamma,f}} dE_\gamma Y^{\gamma P \rightarrow \nu}(E_\gamma, E_\nu) \cdot \sigma_{\gamma P}(E_\gamma) dL_\gamma(E_\gamma, \theta, i) / d\Omega, \quad (4)$$

when the observer has an angle of view, i , with respect to the jet direction. Here, $\Sigma_H(\theta)$ is the column density of target protons in the direction θ , $\sigma_{\gamma P}(E_\gamma)$ is the γP cross-section at a photon energy E_γ and $Y^{\gamma P \rightarrow \nu}(E_\gamma, E_\nu)$ is the ν yield, i.e., the number of neutrinos produced with energy around dE_ν during a collision of a γ -ray with energy in the interval dE_γ with a proton at rest. The cross-section $\sigma_{\gamma P}(E_\gamma)$ was evaluated according to [7] and the yield of neutrinos was taken from [3], where it was calculated with the Monte Carlo program SOPHIA v2.01 [10].

Using equation 2 in expression 4, summing over all directions θ and averaging on the observer's view angle, i , we arrive to the formula

$$L_\nu(E_\nu) dE_\nu = N \cdot \xi(\mathcal{L}_\gamma) \int_{E_{\gamma,i}}^{E_{\gamma,f}} dE_\gamma Y^{\gamma P \rightarrow \nu}(E_\gamma, E_\nu) \cdot \sigma_{\gamma P}(E_\gamma) \left(\frac{E_\gamma}{\text{TeV}} \right)^\alpha e^{-(E_\gamma/10^2 \text{ TeV})}, \quad (5)$$

where

$$\xi(\mathcal{L}_\gamma) = \frac{\int_{\delta\Omega(\mathcal{L}_\gamma)} \int_{4\pi sr} d\Omega_\theta d\Omega_i \Sigma_H(\theta) \cdot \eta(\theta, i)}{\delta\Omega(\mathcal{L}_\gamma)}. \quad (6)$$

In the above formula, we have put a constraint to the direction i of the observer. This restriction is obtained when the luminosity of FR II galaxies, observed from the direction i with photon spectral luminosity \mathcal{L}_γ , is limited to be smaller than 10^{50} ergs/s along the jet axis. This upper limit comes from the observations of FSRQ galaxies with the *Fermi-LAT* telescope [5], which are just FR II AGN's observed along the jet direction according to the unified AGN model [11]. In this way, we integrate the angle i only inside a limited solid angle interval $\delta\Omega(\mathcal{L}_\gamma)$ for which the aforementioned condition is valid. Finally, in equation 5, integration is performed from $E_\gamma = 10^{-0.8}$ (just above the γ -energy threshold for pion photo-production) to 10^6 GeV .

4 Column density

To estimate the column density of the gas and dust at the source, first, we assume that the birth place of the gamma radiation observed from FR II type galaxies is found at the nucleus of the AGN and coincides with the radio core location. In fact, combined multi-wavelength observations of

Structure	$R[\text{pc}]$	$n_H[\text{cm}^{-3}]$
Core	0.03	10^6
BLR region	0.03 – 0.6	$(7.3 \times 10^4) \cdot e^{-(\beta/20^\circ)^2}$
Torus	0.6 – 130	$(3.2 \times 10^2) \cdot e^{-(\beta/20^\circ)^2}$
Inclined disk	0.03 – 80	10^4
Dust lane	$(0.13 - 1.5) \times 10^3$	5.6×10^{-1}
ISM	2×10^3	$0.11/[1 + (7.69 \times 10^{-7}) \cdot r^2]^{0.946}$
Cocoon	$r_- = 15 \times 10^3; r_+ = 60 \times 10^3$	1.9×10^{-4}
Shell	$r_- = 25 \times 10^3; r_+ = 62.5 \times 10^3$	1.4×10^{-2}
Halo	5×10^5	$7.9/r^2$

Table 2: Extension and density distributions of the main gas structures in the model of Cygnus A. Here, r represents the spherical radius, r_- , the semi-minor axis, and r_+ , the semi-major axis of the prolate spheroidal structures. Meanwhile, β is the angle measured from the equatorial plane of the galaxy. It can have only values in the interval $[-20^\circ, 20^\circ]$.

the radio galaxy M87, which hosts a FR I type object, point out that the gamma-ray production site could be located at the nucleus of the AGN [12]. On the other hand, we take Cygnus A as a model for FR II galaxies. The advantage of this choice is that this powerful FR II galaxy has been well studied by different astronomical instruments due to its proximity to the Earth ($z = 0.056$) [13]. Based on reported astronomical observations, we built a simple model of Cygnus A to describe the matter distribution of the main structures of the galaxy (see table 2).

To start with, for the radius of the gamma-source at the nucleus, we take the limit derived from [14] for the compact radio source in Cygnus A. The density was assumed to be 10^6cm^{-3} , which agrees with estimations at the nucleus of AGN's [15]. Observations against the nucleus indicates the presence of a strong X-ray absorber, which could be due to material from the BLR region and a dusty torus. In [16], the torus was modeled with a clumpy circumnuclear disk. Its geometry and density were restricted with radio and IR data. For the torus, we will use the disk model of [16] with a constant radial density, only depending on the angle β respect to the equator of the galaxy, a half opening angle $\sigma = 20^\circ$ (measured from the equatorial plane), an internal radius equal to 0.6pc, an outer radius of 130pc and with axis oriented along the jet direction. We will assume that the BLR region is an inner extension of the torus [17]. Therefore, the BLR region will be described also with a disk with the same geometrical parameters, but with smaller dimensions, particularly with an external radius of 0.6pc. Density is found in such a way that for $\beta = 10^\circ$, which corresponds to the viewing angle of an observer at the Earth [16], the total column depth along the BLR and torus region is $N_H = 2 \times 10^{23} \text{cm}^{-2}$, the value reported by the *Chandra* telescope for the X-ray absorber [21]. We will assume that this column density is equally divided between the BLR region and the torus, since it is unknown exactly what is the exact contribution from each region to the X-ray absorption.

A second disk, tilted 21° with respect to the equatorial plane of the host galaxy, a density $n_H = 10^4 \text{cm}^{-3}$, a radius of 80pc and an opening angle of 14° was also added to our model [18]. It was detected with VLBA HI absorption studies of the core region of Cygnus A [18].

Observations at IR wavelengths also reveal an edge-on oriented biconical structure, which is likely caused by a kpc-scale dust lane characterized by a disk geometry and funnels along the jet axis [19]. In the model of [19], the funnels have an opening angle of 116° , while the disk axis is aligned within 15° with the jet direction. Here, we will incorporate the dust lane with the above configuration in

our model. Besides, for simplicity, we will consider that the disk lies on the equatorial plane of the galaxy. The external diameter and the width of the disk are set to 3kpc [20] and 1.5kpc [21]. On the other hand, we will assume that the inner frontier of the disk coincides with the external radius of the torus. To calculate the density, we take the column density estimated in [21] for the dust lane along the direction to Earth. Taking into account the geometry of the disk and the orientation of the observer, and assuming an homogeneous distribution of the material inside the dust lane, we estimate a density of $5.6 \times 10^{-1} \text{cm}^{-3}$.

The distribution of the interstellar matter up to 2kpc will be described using the same function derived in [22], from optical and IR observations, for the stellar density profile in Cygnus A within the 2kpc region around its nucleus. As in [22], we will assume that matter is spherically distributed in this zone.

Observations suggest that the above structures are surrounded by a cocoon and an external shell with shocked matter [23]. The shapes and densities of these structures were modeled in [24]. Here, we will take the model number 3 of [24], which seems to be in better agreement with observations. According to [24], these structures have a prolate spheroidal shape. The inner (outer) radius of the shell is of the order of 60(62.5)kpc along the semi-major axis, according to the above model, while along the semi-minor axis is 15(25)kpc. On the other hand, in model 3 of [24], the cocoon has a volume of $2.8 \times 10^4 \text{kpc}^3$ and encloses a mass of $1.4 \times 10^8 M_\odot$. From this data the mean cocoon's density is estimated. It is worth to mention that the density of the interstellar region at 2kpc is normalized in such a way that it reproduces the density of the cocoon. An average density of $1.4 \times 10^{-2} \text{cm}^{-3}$ for the shocked region was estimated from the 2D density plots of [24].

Beyond the cocoon and the shell, we found the galactic halo, which is composed of hot and low density gas. This structure has been detected in X-rays. Its emission extends up to 720kpc according to [13]. The electron density has been modeled in [13] from 60kpc to 500kpc from X-ray observations of the halo of Cygnus A. We will use this profile for our proton density, assuming that the proton and electron densities are similar inside the halo. We will apply such an expression only up to 500kpc.

5 Results and Discussion

The $\xi(\mathcal{L}_\gamma)$ factor is presented in figure 1 for different Γ and α parameters. We notice that the $\xi(\mathcal{L}_\gamma)$ factor decreases as the solid angle $\delta\Omega(\mathcal{L}_\gamma)$ gets smaller for high Γ values and \mathcal{L}_γ luminosities. As we will see, that will imply low d-

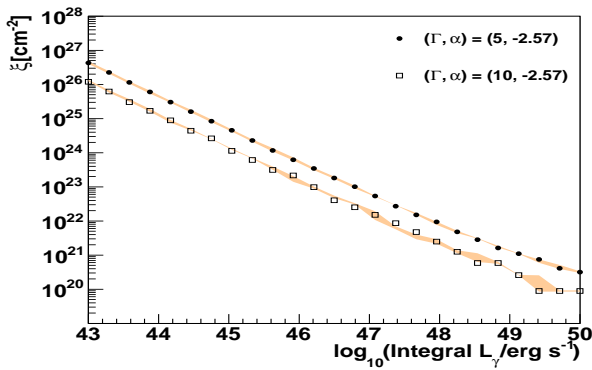


Fig. 1: ξ factor for $\alpha = -2.57$ and $\Gamma = 5$ (circles) and 10 (squares). The bands are generated when the photon index is varied inside its corresponding error interval.

diffuse neutrino fluxes from FR II galaxies for high Lorentz factors. The neutrino background flux as observed at Earth from FR II objects, after ν oscillations, is shown in figure 2. The error band of this flux, calculated by varying the photon index (α) of formula 2 in the interval -2.57 ± 0.18 is also presented. The spectrum is compared with the background of atmospheric neutrinos and the result for FR I type sources [3]. Two fluxes derived from hadronic models [29, 30] and two experimental upper bounds from *ICECUBE* [25] and *Antares* [26], respectively, are also shown. The results show that, although γ -ray FR II emitters seem to be less abundant than the corresponding FR I population, the higher Doppler and beaming factors of FR II galaxies can make their corresponding ν background flux higher than the one for FR I objects. However this difference is not big. Fig. 2 shows that, the investigated neutrino flux from FR II galaxies is too small in comparison with the experimental bounds and the atmospheric background of neutrinos. Neither this feeble flux nor the flux from FR I objects can explain the observed neutrino events detected recently by *ICECUBE* around 1 PeV [31]. Therefore, if these events comes from FR I and FR II objects, their most probable origin would be found at hadronic mechanisms originated by cosmic-ray acceleration.

6 Conclusions

We have shown that in addition to FR I AGN's, FR II type galaxies characterized by γ -ray emission also produce a small neutrino diffuse flux produced by photo-hadronic interactions by γ radiation with the gas and dust at the sources. Both fluxes, in general, are too low to be detected by the modern neutrino telescopes and to explain the last PeV neutrino events detected recently by the *ICECUBE* observatory.

Acknowledgment: This work was partially supported by the *Consejo de la Investigación Científica* of the *Universidad Michoacana* (Project CIC 2012-2013) and *CONACYT* (Project CB-2009-01 132197).

References

[1] J.K: Becker, Phys. Rep. 458 (2008) 173-246.
 [2] M. Böttcher, ASP Conf. Ser. 373, The Central Engine of Active Galactic Nuclei, ed. L.C. Ho and J-M Wang, San Francisco, CA (2007), 169.
 [3] J.C. Arteaga-Velázquez, Astropart. Phys. 37 (2012) 40-50.
 [4] D.A. Evans et al., ApJ 642 (2006) 96-112.

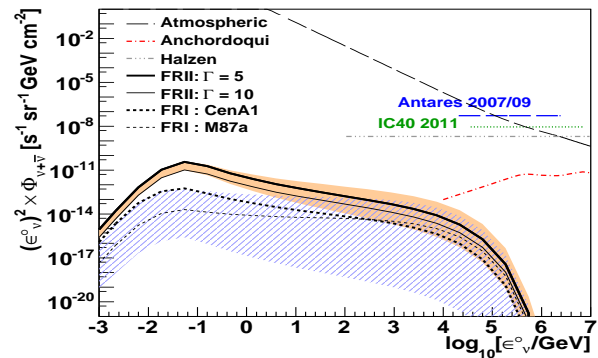


Fig. 2: Diffuse flux of neutrinos (for each type) expected from FR II galaxies assuming different Lorentz factors ($\Gamma = 5, 10$) for the AGN jets. The shadowed band covers the results obtained by varying the photon index inside its error interval for the considered Γ factors. The flux is compared with the expected results for FRI type objects based on a Centaurus A and a M87 models (dotted black lines and hatched area) [3]. ν oscillation is taken into account. The 90% C.L. upper limits on the diffuse ν flux derived by the *ICECUBE* [25] and the *Antares* [26] collaborations are shown. For comparison, the diffuse flux of atmospheric neutrinos (segmented line)[27], including the prompt component from *D*-meson decays [28], is also presented. Two predictions for the diffuse ν flux from AGN's using hadronic models (Anchordoqui [29] and Halzen [30]) are included in the plot.

[5] A.A. Abdo et al., ApJ 720 (2010) 912-922; P. Grandi et al., Proc. of High Energy Phenomena in Relativistic Outflows, arxiv: 1112.2505.
 [6] Y. Inoue, ApJ 733 (2011) 66.
 [7] J. Beringer et al. (Particle Data Group), Phys. Rev. D86 (2012) 010001.
 [8] C. D. Dermer and G. Menon, High Energy Radiation from Black Holes: Gamma Rays, Cosmic Rays, and Neutrinos, Princeton University Press, 2009.
 [9] C.D. Dermer et al., ApJS 109 (1997) 103.
 [10] A. Mücke, R. Engel, J.P. Rachen, R.J. Protheroe, and T. Stanev, Comp. Phys. Commun. 124 (2000) 290,
 [11] C.M. Urry and P. Padovani, PASP 107 (1995) 803.
 [12] The VERTAS Collaboration, the VLBA 43 GHz M87 Monitoring Team, the H.E.S.S. Collaboration and the MAGIC Collaboration, Science 325 (2009) 444.
 [13] D.A. Smith et al., ApJ 565 (2002) 195 - 207.
 [14] R. Barvainis et al., Astron. J. 107, (1994) 1291.
 [15] Z. Abraham et al., Mon. Not. R. Astron. Soc. 375 (2007) 171; D.L. Jones et al., ApJ 534 (2000) 165.
 [16] G.C.Privon et al., ApJ 747 (2012) 46.
 [17] M. Nenkova et al., ApJ.685 (2009) 160-180; Erratum-ibid.723 (2010) 1827.
 [18] C. Struve et al., A&A 513, (2010) A10.
 [19] C.N. Tadhunter et al., ApJ 512 (1999) L91-L94.
 [20] M. J. Bellamy and C. N. Tadhunte, Mon. Not. R. Astron. Soc. 353 (2004) 105-112.
 [21] A.J. Young et al., ApJ 564 (2002) 176.
 [22] C. Tadhunter et al., Mon.Not.Roy.Astron.Soc. 342 (2003) 861.
 [23] C.L. Carilli et al., ApJ 102 (1991) 1691.
 [24] W. G. Mathews et al., ApJ 725 (2010) 1440-1451.
 [25] R. Abbasi et al., Phys. Rev. D 84 (2011) 082001.
 [26] J.A. Aguilar et al., Phys.Lett.B 696 (2011) 16.
 [27] R. Gandhi et al., Phys. Rev. 58D (1998) 093009-1.
 [28] L.V. Volkova, Sov. J. Nucl. Phys. 31, 784 (1980).
 [29] Luis A. Anchordoqui et al., Astrop. Phys. 29 (2008) 1.
 [30] F. Halzen and A. O'Murchadha, arXiv: 0802.0887v2.
 [31] M. G. Aartsen et al., arXiv: 1304.5356.